Transient and sustained effects of stimulus properties on the generation of microsaccades

Roy Amit Sagol School of Neuroscience, Tel Aviv University, Tel Aviv, Israel

Dekel Abeles School of Psychological Sciences, Tel Aviv University, Tel Aviv, Israel

Shlomit Yuval-Greenberg Sagol School of Neuroscience, Tel Aviv University, Tel Aviv, Israel
School of Psychological Sciences, Tel Aviv University, Tel Aviv, Israel

Saccades shift the gaze rapidly every few hundred milliseconds from one fixated location to the next, producing a flow of visual input into the visual system even in the absence of changes in the environment. During fixation, small saccades called *microsaccades* are produced 1–3 times per second, generating a flow of visual input. The characteristics of this visual flow are determined by the timings of the saccades and by the characteristics of the visual stimuli on which they are performed. Previous models of microsaccade generation have accounted for the effects of external stimulation on the production of microsaccades, but they have not considered the effects of the prolonged background stimulus on which microsaccades are performed. The effects of this stimulus on the process of microsaccade generation could be sustained, following its prolonged presentation, or transient, through the visual transients produced by the microsaccades themselves. In four experiments, we varied the properties of the constant displays and examined the resulting modulation of microsaccade properties: their sizes, their timings, and the correlations between properties of consecutive microsaccades. Findings show that displays of higher spatial frequency and contrast produce smaller microsaccades and longer minimal intervals between consecutive microsaccades; and smaller microsaccades are followed by smaller and delayed microsaccades. We explain these findings in light of previous models and suggest a conceptual model by which both sustained and transient effects of the stimulus have central roles in determining the generation of microsaccades.

Introduction

Observers perform high-velocity eye movements called *saccades* around 1–3 times per second. Large saccades are typically produced when attention is shifted from one location on a scene to another; smaller saccades, called *microsaccades*, are produced during periods of fixation (Martinez-Conde, Macknik, & Hubel, 2004) and when fine details are being explored (Ko, Poletti, & Rucci, 2010). Saccades and microsaccades form an oculomotor continuum, as they share the same kinematic properties and are controlled by the same neural structures (Martinez-Conde et al., 2004; Hafed, Goffart, & Krauzlis, 2009). Specifically, oculomotor maps in the superior colliculus are involved in generating saccades of all sizes, as they represent saccade amplitudes continuously: Smaller saccades are represented closer to the rostral pole and larger saccades are represented more caudally (Robinson, 1972; Hafed et al., 2009). During fixation, activity is strongest in the rostral pole, which is the center of the map (Munoz, Dorris, Pare, & Everling, 2000). A saccade is elicited once activity in a certain area of the map surpasses a threshold (Carpenter & Williams, 1995; Hanes & Schall, 1996).

This neurophysiological framework has led to a few theories and models on the generation of microsaccades during fixation. One such conceptual model is the common-field model of microsaccade and saccade generation proposed by Rolfs, Kliegl, and Engbert (2008). This model suggests that microsaccades are generated when fixation-related activity at the rostral center of the superior-colliculus map slightly spreads out

Citation: Amit, R., Abeles, D., & Yuval-Greenberg, S. (2019). Transient and sustained effects of stimulus properties on the generation of microsaccades. *Journal of Vision*, *19*(1):6, 1–23, https://doi.org/10.1167/19.1.6.

https://doi.org/10.1167/19.1.6 Received April 13, 2018; published January 14, 2019 ISSN 1534-7362

to neighboring locations due to local excitation. It proposes that the characteristics of this central distribution of activity explain the direction and amplitude of the generated microsaccades, as they are modified by random noise or nonrandom factors such as spatial attention (Hafed & Clark, 2002; Engbert & Kliegl, 2003; Laubrock, Engbert, & Kliegl, 2005; Yuval-Greenberg, Merriam, & Heeger, 2014; Meyberg, Sinn, Engbert, & Sommer, 2017). The model also accounts for the robust finding that microsaccades are inhibited for ~150 ms following the abrupt presentation of a stimulus (Reingold & Stampe, 2002; Engbert & Kliegl, 2003; Graupner, Velichkovsky, Pannasch, & Marx, 2007; Rolfs, Kliegl, & Engbert, 2008), suggesting that this poststimulus inhibition—which is often followed by a short rebound—is a consequence of a short global inhibition of the entire map triggered by stimulus onset.

Another model, by Engbert and colleagues (Engbert, Mergenthaler, Sinn, & Pikovsky, 2011; Engbert, 2012; Sinn & Engbert, 2016), provided a compatible computational account for the generation of fixational eye movements (drift and microsaccades). According to this model, the generation of these eye movements is based on the concept of a self-avoiding random walk in a potential well, driven by a self-generated activation field. This model captures fundamental properties of the spatial and temporal attributes of microsaccades while providing a combined theoretical framework for microsaccades and drift. In its second version (Engbert, 2012), it integrated the effects of spatial attention and stimulus presentation. In its most recent version (Sinn & Engbert, 2016) the model integrates, among other modifications, a logistic refractory period between consecutive microsaccades, reflecting the observed saccadic refractory period (SRP).

Both the conceptual model by Rolfs, Kliegl, and Engbert and the computational model by Engbert and colleagues integrate the influences of a transient externally presented stimulus, but they do not consider the effects of the static visual display on which microsaccades are generated. There is only little evidence on how the properties of static displays modulate the temporal dynamics of saccades. A few studies focusing on large saccades performed during exploration tasks have examined how the durations of intervals between consecutive saccades (the intersaccadic intervals) are modulated by the type of display being explored. Some of these studies have found longer intersaccadic intervals with higher stimulus intensity (e.g., higher spatial frequency: Rayner, 1998; Ojanpaa, Nasanen, & Kojo, 2002; Ahissar, Arieli, Fried, & Bonneh, 2016); others have found the opposite (Nasanen, Ojanpaa, & Kojo, 2001; Henderson, 2003) or no effects at all (Einhäuser & König, 2003; Itti, 2005). Only one previous study has asked a similar question on microsaccades (Otero-Millan, Troncoso, Macknik, Serrano-Pedraza, & Martinez-Conde, 2008), and found no evidence for an effect of display on their temporal dynamics. However, that was not the main purpose of that study, and the visual properties of the displays were not controlled for.

The static visual display on which microsaccades are performed can theoretically modulate microsaccades through two sources: sustained effects of the cognitive and perceptual state produced by the properties of the static visual display, which may be mediated by various mechanisms including the continuous flow of visual input through ocular drift; and transient effects produced by retinal displacements accompanying occasional microsaccades. These microsaccade-induced retinal displacements produce visual transients, whose properties depend on the properties of the static display on which the inducing microsaccades were performed. Previous studies have demonstrated that such visual transients, produced by saccades, activate the visual system similar to externally presented stimuli (Thickbroom, Knezevič, Carroll, & Mastaglia, 1991; Bair & Keefe, 1998; Kazai & Yagi, 2003; Tse et al., 2010; Kagan & Snodderly, 2017). Since the presentation of external visual stimuli modulates the timing of consecutive microsaccades (Reingold & Stampe, 2002; Engbert & Kliegl, 2003; Graupner et al., 2007; Rolfs, Kliegl, & Engbert, 2008), the visual transients induced by microsaccades are expected to have a similar effect.

Indeed, similar to the stimulus-related modulation of microsaccades, following a microsaccade there is a refractory period of ~150 ms where subsequent microsaccades are less likely to be produced, and this SRP is often followed by a short rebound (Beeler, 1965; Amit, Abeles, Bar-Gad, & Yuval-Greenberg, 2017). It could be hypothesized that this stereotypical temporal pattern is the result of the visual transient produced at the offset of each microsaccade. If this is the case, the implication is that visual transients produced by microsaccades influence the generation of subsequent microsaccades. Such a mechanism would imply that microsaccade generation is modulated by a loop, where the timing of each microsaccade is determined by the visual consequence of the previous one (among other factors). Whereas the stimulus-related modulation of microsaccade rate is discussed in detail by the models of Rolfs, Kliegl, and Engbert as well as Engbert and colleagues, the influences of the visual transients produced at the offset of one microsaccade on the timings of subsequent microsaccades are not thoroughly addressed. The model by Engbert and colleagues integrates statistical dependencies between subsequent microsaccades and includes a transient modulation of the potential at the offset of each microsaccade, but the nature of this transient remains open to interpretation. Here we suggest that the visual transient at the offset of microsaccades is a critical factor in determining subsequent dynamics.

The purpose of the present study is to examine how visual properties (spatial frequency, contrast, and orientation) of a static display modulate the temporal characteristics of microsaccades performed on it. Through theoretical discussion and modeling, we aim to evaluate the potential implications of the visual transients induced by microsaccades on the temporal dynamics of microsaccade generation.

In a series of four experiments we examined how the manipulation of the static display's properties modulates the properties of microsaccades: namely their amplitude (size) and the duration of the refractory period between consecutive saccades (the SRP). The first experiment employed a coarse manipulation of the visual display, contrasting complete darkness, a blank screen, and a complex scene. The second experiment contrasted displays of high and low spatial frequency (SF), and the third experiment contrasted displays of high and low contrast. In these three experiments we consistently found that displays of higher intensities (i.e., higher SF and contrast) resulted in longer inter microsaccade intervals and smaller microsaccades. In a fourth experiment we provide initial evidence for the hypothesis on the involvement of retinal-image displacements. In this experiment we compared microsaccades produced on horizontal and vertical grating backgrounds. Since most microsaccades are horizontal, larger effects with vertical than with horizontal gratings provided initial evidence supporting the involvement of visual transients. We discuss the implications of these findings on the conceptual model by Rolfs, Kliegl, and Engbert and demonstrate how a small modification of the computational model by Engbert and colleagues to account for the display effects on the timings of microsaccades may improve its fit to the experimental data. We conclude that the temporal properties of microsaccades depend on the characteristics of the display backgrounds on which they are performed.

Materials and methods

Participants

Data were collected from 50 participants, all students of Tel-Aviv University who participated in the experiments for payment or course credit. All participants were healthy and reported normal (uncorrected) vision and no history of neurological disorders. Three participants were excluded from analysis: two because of poor gaze monitoring and one due to failure to hold fixation. Following exclusion, there were 11 participants in Experiment 1 (six women, five men; age [$M \pm SD$] = 23.7 ± 2.8), 12 in Experiment 2 (seven women, five men; age = 25.9 ± 3.2), 11 in Experiment 3 (eight women, three men; age = 23.7 ± 4.2), and 13 in Experiment 4 (six women, seven men; age = 24.0 ± 2.6). The experimental protocol was approved by the ethical committees of Tel Aviv University and the School of Psychological Sciences, and experimental sessions were conducted with the written consent of each participant. The eye-tracking data from Experiment 2 were included in a previous publication, focusing on different questions and analysis methods (Amit et al., 2017).

Stimuli

Experiment 1

Near complete darkness was achieved by turning off or covering all sources of light in the experimental chamber, including the computer monitor. The eye tracker's infrared illuminator (940 nm) was slightly visible. In the darkness-fixation conditions, a red laser fixation dot (size 0.2°) was displayed in darkness (on a switched-off computer screen) using a laser pen. In the other fixation conditions, a red fixation cross (size 0.2°) was presented at the center of the screen. Other stimuli included scenery images spanning the entire screen (34° × 26.6°) or a blank midgray screen (34° × 26.6°). In the free-view condition, no fixation cross was presented.

Experiment 2

A red fixation cross (size 0.2°) was presented at the center of a full-contrast checkerboard (size 17° × 13°) centered on a midgray background. Checkerboard SF was 1.67 c/° (high SF) or 0.125 c/° (low SF).

Experiment 3

A red fixation cross (size 0.2°) was presented at the center of a vertical sinusoidal grating (size 17° × 13°) of 1.67 c/°, centered on a midgray background. The grating's Michelson contrast (Michelson, 1927) was either 1 (high contrast) or 0.3 (low contrast).

Experiment 4

A red fixation cross (size 0.2°) was presented at the center of a full-contrast horizontal or vertical sinusoidal grating (size 17° × 13°) centered on a midgray background. The SF of the grating was either 1.67 c/° (high SF) or 0.5 c/° (medium SF).

Procedure

Participants sat, head resting on a headrest, in a sound-attenuated room that was either almost completely dark (darkness condition, Experiment 1) or

dimly lit (the rest of the experiments). They were seated at a distance of 57 cm from a 17-in. CRT display monitor (refresh rate = 60 Hz, resolution = 1,280 × 960) in Experiments 1, 2, and 4; and 97 cm from a 24-in. LCD display monitor (ASUS VG248QE, Taipei, Taiwan; refresh rate = 120 Hz, resolution = 1,920 × 1,080, midgray luminance = 110 cd/m^2) in Experiment 3. We ran Experiment 3 last, but to improve readability we report it here prior to Experiment 4. The reason for the two different setups is that the original CRT monitor was replaced with a newer LCD screen at the end of the (chronologically) third experiment. Eye-tracker calibration was applied at the beginning of each experimental session and then once every four blocks (or more often when needed). In the darkness condition, calibration was performed on a black background after shutting down the lights but before turning off the monitor. A tone was sounded to alert participants when their gaze diverted more than 1.5° away from the central cross for more than 1 s.

Experiment 1

In each block, participants were asked to either fixate a central fixation target (fixation condition) on a static display or free-view the display (free-view condition) for 200 s. The display included either near-complete darkness (darkness condition), a midgray screen (blank condition), or a photo of a scene (scene condition). Each of these six block types repeated three times in a random order (total of 10 min. of recording per condition). To avoid the unexpected effects of large retinal displacements, all analysis—except one where indicated otherwise—was performed only on data from the fixation task.

Experiment 2

Participants were asked to fixate a static checkerboard display for 180 s. In separate blocks (randomly distributed), the displays were of either high or low SF, with each block type appearing six times during the session. Once every 5–22 s (randomly) a black screen replaced the checkerboard for 16.7 ms (one monitor refresh). Participants were instructed to silently count the number of black-screen appearances and report this number at the end of each block.

Experiment 3

This was the same as Experiment 2 but with contrast modulation (high/low) instead of the SF modulation.

Experiment 4

This was the same as Experiment 2 but with a manipulation of orientation (vertical/horizontal) in addition to the manipulation of SF (high/medium). Gratings with high or medium SF were presented in separate blocks, with each block type appearing eight times during the session. The grating image flipped every 5–22 s ($M = 13.5$ s) from vertical to horizontal or vice versa, replacing the black transients of the previous experiments. The new orientation remained until the next flip or the end of the block, and data were analyzed on these segments according to the presented orientation. Participants were asked to count the orientation flips and report the number at the end of each block.

Eye tracking

Eye movements were monitored in all four experiments using a remote infrared video-oculographic system (EyeLink 1000 Plus; SR Research, Ottawa, Canada) with a spatial resolution of ≤0.01° and average accuracy of 0.25°–0.5° when using a headrest (as reported by the manufacturer). Raw gaze positions, sampled at 1000 Hz, were converted into degrees of visual angle using a 9-point grid calibration, performed at the start of each experimental block. Some doubts have been previously raised regarding the adequacy of video-oculographic eye trackers for measuring microsaccades (Poletti & Rucci, 2016). However, their performance in detecting miniature fixational eye movements has been found to be comparable to that of the invasive search-coil technique, considered the gold standard in this field (McCamy et al., 2015). Compared with other commercial devices, including the dual-Purkinje-image eye tracker, the EyeLink device has been found to be among the highest in tracking precision (Wang, Mulvey, Pelz, & Holmqvist, 2016).

Microsaccade detection

Microsaccades were detected using a published algorithm (Engbert and Mergenthaler, 2006). An elliptic threshold criterion for microsaccade detection was determined in 2-D velocity space based on the horizontal and vertical velocities of the eye movement. Specifically, we set the threshold to be six times the standard deviation of the eye-movement velocity, using a median-based estimate of the standard deviation (Engbert & Mergenthaler, 2006). A microsaccade onset was detected only if six or more consecutive velocity samples were outside the ellipse.

Saccades are often followed by an overshoot, which resembles a small saccade. To avoid including such overshoots in the analysis, we included saccades only if they were not preceded by another saccade for at

least 50 ms. Saccade amplitude (size) was calculated as the Euclidean distance between gaze position at the onset of the saccade and gaze position at its offset. Unless indicated otherwise, our analysis focused on microsaccades, defined as saccades with amplitude smaller than 1.5°. The same pattern of results was evident when we used a threshold of 1° instead of 1.5°. The validity of the detected microsaccades was checked by verifying that they followed the main sequence of saccades. This was done by showing a linear correlation (Pearson r) between the logs of velocity and amplitude (Zuber, Stark, & Cook, 1965; Bahill, Clark, & Stark, 1975).

Measuring the SRP

We constructed the probability density functions of the inter microsaccade intervals (IMSIs) by examining the intervals between all pairs of consecutive microsaccades. In Experiment 1 we analyzed all pairs of microsaccades occurring during the continuous blocks of 200 s. In Experiments 2–4, we analyzed the intervals between pairs of consecutive microsaccades occurring during segments of gaze data starting 1 s after the block onset or after a transient change of the display and ending at the end of the block or at the next display change. All pairs of microsaccades in these segments were included unless there was a blink or a large saccade between them. For each participant and condition, we constructed an IMSI distribution and fitted it with an ex-Gaussian function using a published algorithm (Lacouture & Cousineau, 2008). We then extracted the parameter μ representing the mean of its Gaussian component. These μ values were used to estimate the duration of the SRP.

Square wave jerks

Square wave jerks (SWJs) are the combination of one small saccade that moves the eye away from the fixation target and, after a short period, a second corrective saccade directed back toward the fixation target (Otero-Millan et al., 2011). We focused here on SWJs that are within the microsaccade amplitude threshold. Saccades were defined as part of a SWJ pair if they were directed to opposite directions (diverged by 180° ± 30°), their amplitudes differed by no more than 0.3°, and they occurred less than 400 ms apart. These detection criteria are inclusive and liberal relative to previous publications because our goal was to minimize detection misses as much as possible.

Statistics

The SRPs (μ values of the fitted ex-Gaussian distributions) and saccade amplitudes were compared between conditions using repeated-measures analyses of variance (ANOVAs) or paired-sample t tests. The assumption of sphericity was tested, when applicable, using Mauchly's test. When Mauchly's test was found significant ($p < 0.05$), the Greenhouse–Geisser corrected F and p values are reported, along with the original degrees of freedom and the epsilon value. All the statistical tests performed were two-tailed.

Individual correlations were examined per participant and condition by applying the Fisher's transform on the Pearson correlation coefficients. The significance of these individual correlations was then measured using a t test, and p values were corrected for multiple comparisons (according to the number of examined participants and conditions) using the false discovery rate (Yekutieli & Benjamini, 1999). The corrected p values (pFDR) are reported. Grand average correlations across participants were calculated by taking the Fisher's transform of each individual r coefficient, averaging them, and applying the inverse Fisher's transform on the result (Silver & Dunlap, 1987). When r correlation coefficients are compared across participants, the comparison is made on the Fisher-transformed coefficients. For this correlation analysis we excluded a few outlier pairs of microsaccades that were separated by long intervals. Since the IMSI distribution is typically centered around ~250 ms, we chose to exclude IMSIs that were longer than 1 s and consequently at the extreme end of the distribution's exponential tail. Choosing this threshold resulted in the exclusion of 12.7% ± 8.6% ($M \pm SD$) of microsaccades.

A bootstrap analysis was performed to test whether the observed condition effects prevail after microsaccade amplitudes are controlled for. Microsaccades of different conditions were sequentially binned to 100 bins, according to their amplitudes. For each of these amplitude bins, we chose n to be the number of microsaccades in the smaller bin among the two conditions. In each iteration of the bootstrap procedure, n microsaccades were sampled with return from each bin, and these microsaccades were pooled together to create a new distribution with equalized amplitudes. We then fitted an ex-Gaussian to the remaining IMSIs and extracted its μ parameters for each condition, as was already described for the main analysis. These difference values were sorted and the low and high 2.5% values (in places 25 and 975 of the sorted array) were reported as the 95% confidence interval around the mean difference. When zero was outside this confidence interval we concluded that there was evidence supporting the existence of

condition effects that are independent of microsaccade amplitudes.

Computational model

In a series of publications (Engbert et al. 2011; Engbert, 2012; Sinn & Engbert, 2016), Engbert and colleagues proposed a model to describe the temporal and spatial dynamics of fixational eye movements as they are represented in the oculomotor maps of the superior colliculus. This model has been successful in reproducing a wide range of findings on drift and microsaccades, but it does not explicitly address the effect of the intensity of the visual transients produced at the offset of microsaccades on the temporal dynamics of microsaccades and on the SRP. We based our model on the third and latest version of Engbert's model (Sinn & Engbert, 2016), which we modified to reflect the effects of the intensity of visual input on the intervals between consecutive microsaccades.

The original model by Engbert and colleagues was based on a self-avoiding random walk on a finite grid of dimension $L \times L$. The walker represents the gaze position, changing over time, and the grid represents the visual field. In each time step t, the walker moves from its current location (i, j) to a new location. This motion is driven by the movement potential on the grid. This movement potential $E(i, j, t)$ at position (i, j) and time point t is defined as the sum of two values: the potential map $u(i, j)$, a constant map with a symmetrical trough at the center of fixation (i_0, j_0) to simulate the fixation task; and the activation map $h_{i,j}(t)$, a map simulating activity in the motor map of the superior colliculus. The potential map is defined as

$$u(i,j) = aL\left(\left(\frac{i-i_0}{i_0}\right)^2 + \left(\frac{j-j_0}{j_0}\right)^2\right), \quad (1)$$

where a represents the steepness of the trough at fixation.

The activation map is determined at each step according to the current position of the walker. When the walker is on position (i, j), activation at this position is increased by 1 and activation in all other positions decays:

$$h(k,l) = \begin{cases} k,l = i,\ j,\ h_{k,l}(t-1) + 1 \\ k,l \neq i,\ j,\ h_{k,l}(t) = (1-\varepsilon)\cdot h_{k,l}(t)(t-1) \end{cases}. \quad (2)$$

The walker can walk slowly (i.e., one position on the grid at each time step) or quickly (i.e., more than one position at each time step). The slow movements represent eye drift and the faster movements represent microsaccades. The type of motion produced in each time step is determined by the movement potential $E(i, j)$.

As long as $E(i, j)$ at the current position is below a critical value E_{crit}, the walker will move to the position with the lowest movement potential among the four adjacent positions to its current position on the grid $(i\pm1, j\pm1)$. This produces a slow drift. However, when $E(i, j)$ is larger than E_{crit}, the walker jumps to the position of the global minimum of the movement potential. This simulates a microsaccade.

In the third and most recent version of the model, Sinn and Engbert (2016) proposed a few modifications to the original version. Especially relevant to the current study is the addition of an inhibition period between consecutive microsaccades. This inhibition was implemented by creating a time-dependent potential through multiplying the potential $E(i, j)$ with a time-dependent factor, $a_p(t)$ and transiently increasing the critical threshold E_{crit}:

$$E_{crit}(t) = \frac{1}{1 + \lambda_2 \cdot \exp(-\rho_2 \cdot t^2)} \quad (3)$$

$$E(i,j,t) = E(i,j) \cdot a_p(t), \quad (4)$$

where t is the time since the last saccade and

$$a_p(t) = \frac{1}{1 + \lambda_1 \cdot \exp(-\rho_1 \cdot t^2)}. \quad (5)$$

This modification produces a refractory period that decays exponentially with time following the saccadic event but is not modulated by visual content.

We integrated two changes in the model's implementation of the SRP. First, to account for the finding that the IMSIs follow an ex-Gaussian distribution, we modified the SRP to be randomly sampled out of a Gaussian distribution rather than the logistic SRP used before. Note that the underlying assumption of this modeling choice is that the microsaccades are not a purely stochastic process but are modulated by nonstochastic factors. Second, to fit the findings that higher SF and contrast induce longer IMSIs, our modified model determines the SRP duration according to the SF and the contrast of the retinal image. In the revised model, E_{crit} is constant and does not change after each saccade, and potential $E(i, j)$ is not multiplied by a_p. Alternatively, a saccadic refractory period T is sampled from a normal distribution $N(\mu, \sigma)$. The mean μ of this distribution is estimated as the sum of two parameters: μ_0, which represents the individual observer's SRP, and μ_{ret}, which represents the effect of stimulus properties (e.g., SF) on the SRP. Separating these two parameters is necessary to account for the observation that in addition to the stimulation effects there are substantial individual differences in the durations of the SRP. Together,

these two parameters define μ:

$$\mu = \mu_0 + \mu_{ret}. \quad (6)$$

The μ_{ret} parameter was set to 0 in the low-SF condition and fitted to the data for the high-SF condition (see later). These changes reduced the number of parameters by two relative to the original model: instead of E_{crit}, λ_1, ρ_1, λ_2, and ρ_2, we now have only E_{crit}, μ, and σ, fitted for each observer and condition. Relaxation rate ε and potential well steepness a were set to 0.001 and 1, respectively, as in the original model (Sinn & Engbert, 2016).

Parameters of both the original model and our revised model were fitted to the experimental data by a systematic search through parameter space. For the original model, the reported parameters were tested along with a range of ±10 standard errors of each parameter (in gaps of 0.5 standard errors), and in addition with the following parameter subspace: $7.88 \leq E_{crit} \leq 7.99$, with intervals of 0.01; $2 \times 10^{-4} \leq \rho_1 \leq 4 \times 10^{-3}$, with intervals of 4×10^{-4}; $1 \times 10^{-6} \leq \rho_2 \leq 2.5 \times 10^{-5}$, with intervals of 1×10^{-6}; $1.4 \leq \lambda_1 \leq 4.3$ with intervals of 0.2; and $1 \leq \lambda_2 \leq 3$ with intervals of 0.1. For the revised model, the tested parameters were $7.88 \leq E_{crit} \leq 7.99$ with intervals of 0.01; $50 \leq \mu \leq 400$ with intervals of 5; $10 \leq \sigma \leq 120$, with intervals of 10. These parameter spaces were chosen to make sure that any possible parameter set is well within the tested range. Goodness of fit (GOF) for each parameter set was calculated by a chi-square test between the resulting model's IMSI distribution and the original one. IMSIs between 0 and 1,000 ms were divided into k equiprobable bins. The value of k was chosen to be the integer nearest to $1.88 \times n^{2/5}$, where n is the number of samples in the original IMSI distribution according to a standard procedure (D'Agostino, 1986). The parameter set resulting in lowest chi-square statistic was chosen for each data set.

Results

Experiment 1

Saccade properties

The relation between the amplitudes and velocities of the saccades followed the main sequence of saccades for all participants and conditions (correlation between amplitude and velocity: $r > 0.86$ for all data sets and all saccade sizes; $r > 0.85$ for microsaccades alone). In the fixation task, nearly all saccades (>93%) were defined as microsaccades (smaller than 1.5°), indicating that observers complied with the fixation instruction. In contrast, in the free-view task only 45.2% of saccades were defined as microsaccades. To avoid the effects of large retinal displacements, all the following analyses were performed on microsaccades only and on the fixation task only, unless indicated otherwise. The average number of analyzed microsaccades for an individual data set was 5,356 (SD = 1,360, range = 3,153–8,292).

Distribution of IMSIs

The statistical properties of discrete events, such as microsaccades, can be examined through the distribution of the intervals between two consecutive events. For events that occur randomly in time (Poisson processes), the inter event intervals follow an exponential distribution. Any other distribution of intervals suggests a nonrandom process. Consistent with previous findings (Otero-Millan et al., 2008; Bosman, Womelsdorf, Desimone, & Fries, 2009), we found that the IMSI distributions fit an ex-Gaussian (a convolution of a Gaussian and an exponential function) better than a variety of other distributions, including exponential. To verify this, we calculated the Bayesian information criterion (BIC) for GOF (Kass & Raftery, 1995) for all IMSI distributions, fitted with several different probability distribution functions. The ex-Gaussian distribution showed the highest mean GOF (lowest BIC) across observers ($M = 4.95 \times 10^4$, $SD = 2.41 \times 10^3$), compared with an exponential distribution ($M = 5.1 \times 10^4$, $SD = 2.49 \times 10^4$, $p = 0.00041$), a Gaussian distribution ($M = 5.26 \times 10^4$, $SD = 2.59 \times 10^4$, $p = 0.00028$), and a gamma distribution ($M = 5 \times 10^4$, $SD = 2.4 \times 10^4$, $p = 0.00079$). We conclude that the intervals between microsaccades do not follow an exponential distribution, and therefore microsaccades are interdependent and are not a pure Poisson process.

Display effect on IMSIs

The μ parameter of the ex-Gaussian distribution reflects the mean of its Gaussian component. Considering the ex-Gaussian pattern of an inhibition followed by a rebound, μ represents the duration of the inhibition, or the SRP. To test our hypothesis that the duration of the SRP is affected by the display, we compared the fitted μ values across the display conditions.

A one-way repeated-measures ANOVA was performed on fixation data with display (darkness, blank, and scene) as an independent factor and μ as a dependent measure. There was an effect (Figure 1A–1C) of display, $F(2, 20) = 10.73$, $p < 0.001$, caused by a smaller μ for darkness relative to blank, $F(1, 10) = 5.45$, $p = 0.042$, and a smaller μ for blank relative to scene, $F(1, 10) = 5.25$, $p = 0.045$. When analyzing all saccades instead of only microsaccades, we find the same pattern of results: a significant display effect, $F(2, 20) = 16.17$, $p < 0.0001$, with μ smaller for darkness than for blank, $F(1, 10) = 8.13$, $p = 0.0172$, and smaller for blank than for scene, $F(1, 10) = 9.96$, $p = 0.010$.

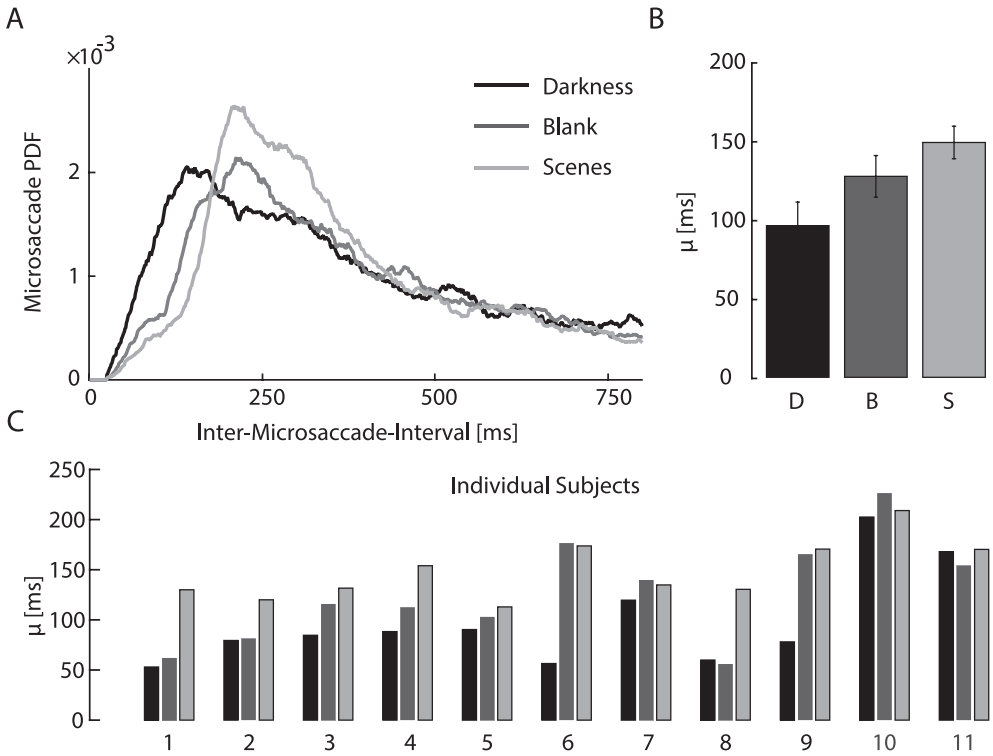

Figure 1. Results of Experiment 1, fixation task. (A) Inter microsaccade interval distributions (probability density functions) of three different conditions. (B) Grand average ($n = 11$) of fitted μ parameter for each of the three display conditions: darkness (D), blank (B), and scene (S). Error bars represent 95% within-subject confidence intervals (Cousineau, 2005). (C) Fitted μ parameter for individual participants in all conditions.

It could have been suggested that the effects of display on the μ value are mediated by differences in microsaccade rate between the conditions: There might have been more microsaccades for a less intense display, and this may have induced shorter IMSIs and consequently shorter SRPs. We find no evidence for this. In the fixation condition there was no significant difference in the rate of microsaccades between the displays, $F(2, 20) = 0.25$, $p = 0.78$. This indicates that the IMSIs in the ex-Gaussian distribution are characterized by a "heavy" exponential tail, resulting from many long IMSIs. Consequently, the μ parameter of the IMSIs in the ex-Gaussian distribution is substantially smaller than the mean IMSI. Moreover, a previous study (McCamy, Otero-Millan, Di Stasi, Macknik, & Martinez-Conde, 2014) has shown that there are more, rather than fewer, microsaccades on more informative regions of a display. Therefore, the prediction on the relation between the display and microsaccade rate should have been the opposite: shorter IMSIs (more microsaccades) for more intense stimuli.

Microsaccade amplitudes

We tested differences in microsaccade amplitude between the display conditions. A one-way repeated-measures ANOVA was conducted with display (darkness, blank, and scene) as an independent factor and mean amplitude as a dependent measure. There was a significant effect of condition, $F(2, 20) = 47.9$, $p < 10^{-5}$. Average microsaccade size ($M \pm SD$) was 0.52° ± 0.12° for darkness; 0.38° ± 0.10° for blank, and 0.38° ± 0.10° for scenes. Planned contrasts showed a significant difference between darkness and blank, $F(1, 10) = 85.7$, $p < 10^{-5,}$ but none between scene and blank—scene > blank: $F(1, 10) = 0.086$, $p = 0.76$ (Figure 2A).

Additionally, we calculated the correlations between the amplitudes of consecutive microsaccades (Figure 2B). Correlations calculated individually for each participant were found to be significantly larger than zero across participants in all display conditions of the fixation task—darkness: mean $r = 0.28$, $t(10) = 6.9$, $p < 10^{-4}$; blank: mean $r = 0.30$, $t(10) = 9.62$, $p < 10^{-5}$; scene: mean $r = 0.34$, $t(10) = 10.74$, $p < 10^{-6}$ (see individual correlations in Table 1).

We examined the possibility that the correlation of amplitudes between consecutive microsaccades could be explained by SWJs, small saccades away from fixation which are closely followed by a corrective saccade of a similar sizes. We repeated this analysis after excluding the SWJs defined by a liberal inclusion criterion, which is expected to minimize misses (see Materials and methods). Following the exclusion of SWJs, the correlations were substantially reduced,

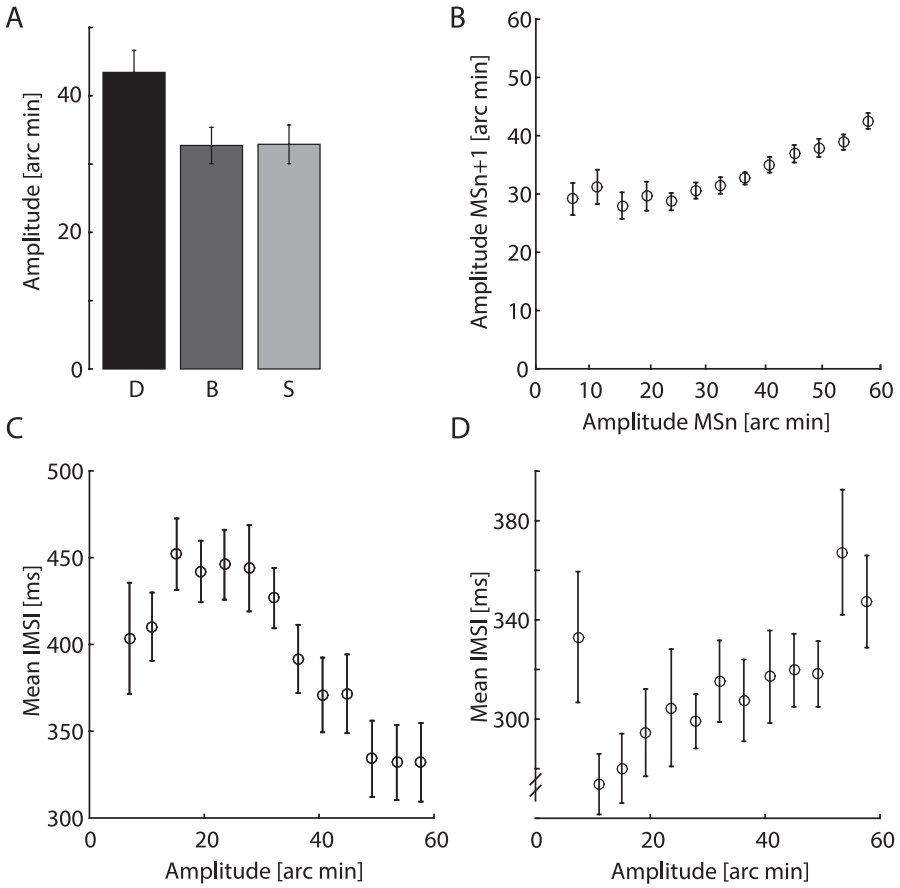

Figure 2. Amplitudes of saccades in Experiment 1. (A) Mean amplitudes of microsaccades in the three display conditions of the fixation task. Error bars represent within-subject standard error of the mean. (B) Correlation between amplitudes of consecutive microsaccades. For the purpose of display, microsaccades from the blank and scene conditions were divided into 15 equidistant bins by size (*x* axis). Circles represent mean amplitude of the consecutive microsaccade, averaged across the microsaccades in each bin and across participants. Error bars denote the standard errors across participants. (C) Correlation between the amplitude of a microsaccade and the following inter microsaccade interval, in the fixation condition. For the purpose of display, microsaccades from the blank and scene conditions were divided into 15 equidistant bins by size (*x* axis). Circles represent mean inter microsaccade intervals and error bars denote the standard errors across participants. (D) Same analysis as in (C) but in the free-view condition, depicting the duration of intervals between microsaccades and large saccades.

which was expected considering the definition of SWJ as consecutive saccades of similar sizes. However, even after exclusion of the SWJs, the correlations between sizes of consecutive saccades were still significantly positive across participants—darkness: mean $r = 0.19$, $t(10) = 4.78$, $p < 10^{-3}$; blank: mean $r = 0.20$, $t(10) = 5.07$, $p < 10^{-3}$; scene: mean $r = 0.24$, $t(10) = 8.64$, $p < 10^{-5}$. We conclude that consecutive microsaccades are correlated in amplitude and that this correlation cannot be explained by corrective saccades alone.

Correlation between microsaccade amplitudes and IMSIs

We tested the correlations between the amplitude of each microsaccade and the duration until the next microsaccade. These correlations were calculated separately for each participant, task, and display, and transformed into *z* scores. The correlations were found to be significantly negative across participants in the blank and scene conditions—blank: mean $r = -0.24$, $t(10) = 7.15$, $p < 10^{-4}$; scene: mean $r = -0.21$, $t(10) = 10.08$, $p < 10^{-5}$ (Figure 2C)—but not in the darkness condition: mean $r = -0.10$, $t(10) = -1.87$, $p = 0.09$ (see individual correlations in Table 1). This shows that smaller microsaccades tended to induce longer IMSIs than larger microsaccades in light conditions (blank and scene), but not in darkness (Figure 2C). The same qualitative effect was found after excluding SWJs—blank: mean $r = -0.21$, $t(10) = 6.42$, $p < 10^{-4}$; scene: mean $r = -0.16$, $t(10) = 8.20$, $p < 10^{-5}$.

In a previous study, Rolfs, Laubrock, and Kliegl (2008) found an opposite, positive correlation between the amplitude of microsaccades and the time interval until a consecutive large saccade. To examine this, we included a free-view condition, where there were

Experiment	Condition	Number of participants (total)	Number of participants with significant (pFDR < 0.05) amplitude–amplitude correlations	Number of participants with significant (pFDR < 0.05) amplitude–IMSI correlations
1	Darkness	11	11 positive	0 positive
			0 negative	5 negative
	Blank	11	11 positive	0 positive
			0 negative	11 negative
	Scene	11	11 positive	0 positive
			0 negative	11 negative
2	Low SF	12	12 positive	0 positive
			0 negative	11 negative
	High SF	12	11 positive	0 positive
			0 negative	11 negative
3	Low cont.	11	11 positive	0 positive
			0 negative	10 negative
	High cont.	11	11 positive	0 positive
			0 negative	10 negative
4	High SF, horizontal	13	13 positive	0 positive
			0 negative	9 negative
	High SF, vertical	13	13 positive	0 positive
			0 negative	10 negative
	Medium SF, horizontal	13	13 positive	0 positive
			0 negative	9 negative
	Medium SF, vertical	13	13 positive	0 positive
			0 negative	11 negative

Table 1. Summary of within-subject correlations. For each experiment and display condition, we report the number of participants with significant negative or positive correlations between amplitudes of consecutive microsaccades and between the amplitude of one microsaccade and the duration of the interval until the next microsaccade. *Notes*: Correlations are calculated within subjects and across pairs of consecutive microsaccades. Correlations of Experiment 1 were based on data from the fixation condition. IMSI = inter microsaccade interval; SF = spatial frequency; cont. = contrast.

relatively few IMSIs (intervals where a microsaccade followed a microsaccade) but many intervals where a large saccade followed a microsaccade. In this condition we examined the correlations between the amplitude of a microsaccade and the time until the next large (>1.5°) saccade. Consistent with Rolfs, Laubrock, and Kliegl, we found significantly positive correlations across participants in the blank and scene conditions—blank: mean $r = 0.14$, $t(10) = 4.46$, $p = 0.0012$; scene: mean $r = 0.12$, $t(10) = 4.36$, $p = 0.0014$ (Figure 2D)—but not in the darkness condition: mean $r = -0.03$, $t(10) = 0.97$, $p = 0.35$. The correlations were less consistent in individual participants than the negative correlations reported for IMSIs: They were positive in 10/11 and 11/11 participants in the blank and scene conditions, respectively, and significant for 4/11 (pFDR < 0.05) in both conditions (7/11 when collapsing the two conditions). In the darkness condition, only 5/11 correlations were positive, and none were significant.

Summary

Results of Experiment 1 show that the IMSI distribution fits an ex-Gaussian distribution better than an exponential distribution. This is consistent with the view that microsaccades are at least partially governed by a nonrandom process and are interdependent (Sinn & Engbert, 2016; Amit et al., 2017). By analyzing the IMSI distributions, we demonstrated the existence of an SRP of approximately 100–150 ms, consistent with previous reports (Nachmias, 1961; Beeler, 1965; Carpenter, 1977; Otero-Millan et al., 2008; Sinn & Engbert, 2016).

The type of constant display on which microsaccades were performed modulates both the SRP between microsaccades and their amplitudes: Longer IMSIs and smaller microsaccades were found for displays of higher intensity. Additionally, there was a negative correlation between the amplitudes of microsaccades during fixation and the IMSI following them: Smaller microsaccades tended to be followed by longer IMSIs. Using the free-view condition we were able to measure larger saccades and estimate the correlation between the amplitude of a microsaccade and the time until the next large saccade. In this case, an opposite, positive, correlation was observed. This positive correlation is consistent with previous findings (Rolfs, Laubrock, &

Kliegl, 2008), and its implications are discussed in detail in the Discussion.

The different components of the triangular relation between visual display, microsaccade amplitudes, and IMSIs could either be interdependent or independent. The correlation between saccade amplitude and IMSIs, combined with the effect of display on amplitude, could be the sole source of the effect of display on IMSIs. Alternatively, the two links can be independent—that is, display may modulate IMSIs regardless of the amplitude of the preceding microsaccade. The causal nature of these links is discussed later.

Experiment 2

In Experiment 1 we took a fairly crude approach to studying the effects of visual intensity on the temporal statistical properties of microsaccades. The purpose of the next two experiments was to refine the visual low-level properties which mediate the observed intensity effect. In Experiment 2 we tested whether increasing the SF of the display extends the SRP; in Experiment 3 we tested whether increasing the contrast of the display results in a similar effect.

Saccade properties

Saccades followed the main sequence for all participants in both conditions (correlation between amplitude and velocity: $r > 0.87$ for all data sets). The average number of analyzed microsaccades for an individual data set was 2,897 ($SD = 1{,}046$, range = 1,429–4,613).

Distribution of IMSIs

The ex-Gaussian distribution showed the highest mean GOF (lowest BIC) across observers ($M = 1.55 \times 10^4$, $SD = 6.58 \times 10^3$), compared with an exponential distribution ($M = 1.62 \times 10^4$, $SD = 7.3 \times 10^3$, $p = 0.001$), a Gaussian distribution ($M = 1.63 \times 10^4$, $SD = 7.07 \times 10^3$, $p = 0.0001$), and a gamma distribution ($M = 1.57 \times 10^4$, $SD = 6.9 \times 10^3$, $p = 0.003$).

Display effects on IMSIs

As predicted, the μ values (Figure 3B–3C) were higher for the high-SF condition compared to the low-SF condition, $t(11) = 3.36$, $p = 0.0064$. It is unlikely that the microsaccade rate mediated this effect, because there was no significant difference in the rate of microsaccades between the two display conditions—high SF: $M = 1.31$ Hz; low SF: $M = 1.33$ Hz; $t(11) = -0.3$, $p = 0.76$.

Microsaccade amplitudes

The difference between conditions in saccade sizes (Figure 3D) was significant, $t(11) = 3.81$, $p = 0.0029$), with smaller amplitudes ($M \pm SD$) for the high-SF condition than the low-SF condition—high: 0.36° ± 0.14°; low: 0.44° ± 0.17°. As in Experiment 1, the correlations between the sizes of consecutive microsaccades were significantly positive across participants in both conditions—high SF: mean $r = 0.22$, $t(11) = 4.80$, $p < 10^{-3}$; low SF: mean $r = 0.27$, $t(11) = 7.18$, $p < 10^{-4}$ (see individual correlations in Table 1). Smaller microsaccades tended to be followed by smaller microsaccades (Figure 3F). As in Experiment 1, correlations between consecutive saccade sizes were lower but still significant after SWJs were excluded from the analysis—high SF: mean $r = 0.13$, $t(11) = 4.73$, $p < 0.001$; low SF: mean $r = 0.16$, $t(11) = 6.10$, $p < 10^{-4}$.

Correlation between amplitudes and IMSIs

Correlations between microsaccade amplitude and the following IMSI were significantly negative across participants in both conditions—high SF: mean $r = -0.16$, $t(11) = 7.17$, $p < 10^{-4}$; low SF: mean $r = -0.17$, $t(11) = 5.95$, $p < 10^{-3}$ (see individual correlations in Table 1). This indicates that IMSIs were longer following smaller microsaccades than following larger ones (Figure 3E).

Following the finding of a correlation between microsaccade amplitude and IMSI, it could be suggested that the effect of the display on IMSIs (described earlier) is simply caused by its effect on amplitude: A higher SF display results in smaller saccades, and smaller saccades are associated with longer IMSI. These two links could suffice to explain the modulation of IMSIs by display. To test the hypothesis that the SF of the display modulates the IMSIs independently of the effect of display on microsaccade amplitudes, we balanced microsaccade amplitudes across conditions using an iterative bootstrapping procedure. We examined the display effects (high-SF μ − low-SF μ) in these unbiased data sets and constructed the 95% confidence interval of the effect (see Materials and methods for more details). The resulting confidence interval [5.63, 14.55] did not include the zero value, supporting the existence of an SF effect on IMSI that is independent of microsaccade amplitude.

Summary

The results of Experiment 2 were consistent with Experiment 1 and showed that a high-SF display induced smaller microsaccades and longer IMSI than a low-SF display, that there is a positive correlation between the amplitude of one microsaccade and that of

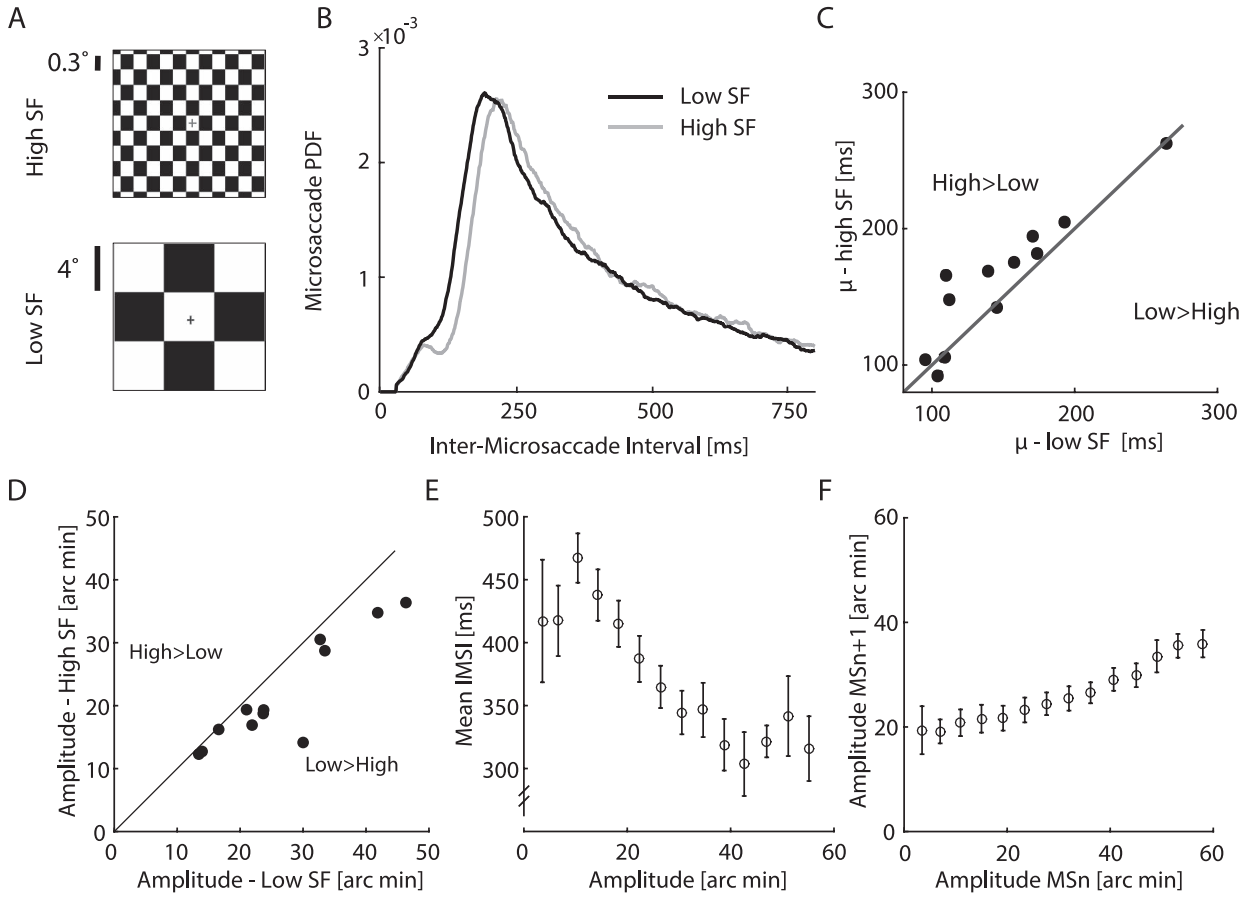

Figure 3. Results of Experiment 2. (A) Visual displays. (B) Inter microsaccade interval distributions for high- and low-spatial-frequency displays. (C) Fitted μ parameter for all participants in both conditions. The identity line represents equal μ values for high and low spatial frequency. (D) Mean microsaccade amplitude for all participants in both conditions. The identity line represents equal μ values for high and low spatial frequency. (E) Correlation between amplitude of a microsaccade and the following inter microsaccade interval. For the purpose of display, microsaccades were divided into 15 equidistant bins by size (*x* axis). Circles represent mean inter microsaccade intervals and error bars denote the standard errors across participants. (F) Correlation between amplitudes of consecutive microsaccades. For the purpose of display, microsaccades were divided into 15 equidistant bins by size (*x* axis). Circles represent mean amplitude of the consecutive microsaccade, averaged across the microsaccades in each bin and across participants. Error bars denote the standard errors across participants.

the next, and that smaller microsaccades tend to be followed by longer IMSIs. When microsaccade size was controlled for, the effect of display on IMSI was not eliminated, suggesting the existence of a direct link between display and IMSI which is independent of microsaccade amplitudes.

Experiment 3

Saccade properties

Saccades followed the main sequence for all participants (correlation between amplitude and velocity: mean $r = 0.96$, $r > 0.89$ for all data sets). The average number of analyzed microsaccades for an individual data set was 1,664 ($SD = 269$, range = 1,265–2,133).

Distribution of IMSIs

The ex-Gaussian distribution showed the highest mean GOF (lowest BIC) across observers ($M = 9.92 \times 10^3$, $SD = 1.62 \times 10^3$), compared with an exponential distribution ($M = 1.02 \times 10^4$, $SD = 1.74 \times 10^3$, $p < 0.001$), a Gaussian distribution ($M = 1.00 \times 10^4$, $SD = 1.62 \times 10^3$, $p < 0.001$), and a gamma distribution ($M = 1.04 \times 10^4$, $SD = 1.64 \times 10^3$, $p < 0.001$).

Display effects on IMSIs

The μ values of the fitted ex-Gaussian were higher for the high-contrast compared to the low-contrast display, $t(10) = 2.53$, $p = 0.0295$ (Figure 4B). Microsaccade-rate is an unlikely explanation for this effect, as there was no significant difference in the rate of microsaccades between the two display conditions—

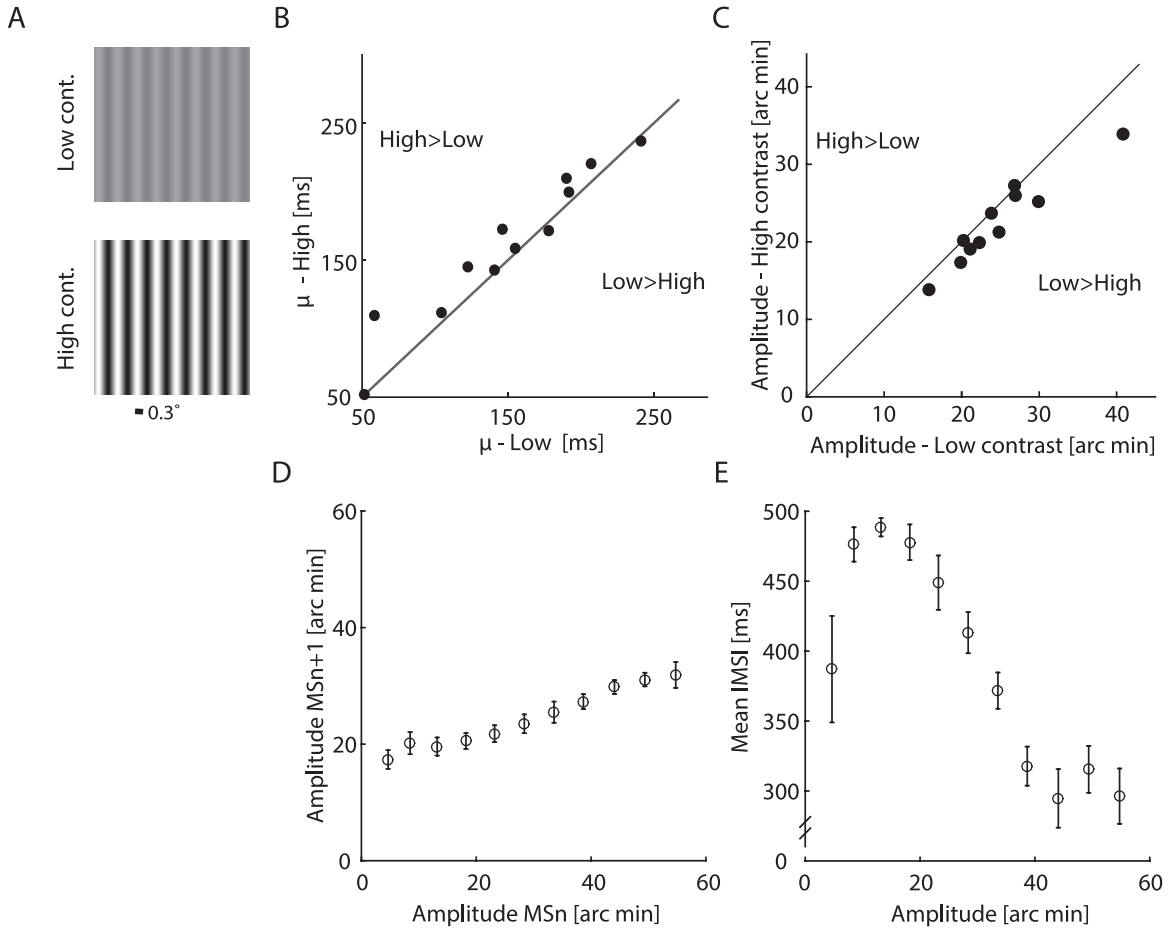

Figure 4. Summary of results for Experiment 3. (A) Visual displays. (B) Fitted μ parameter for each individual in each condition. The identity line represents equal μ values for high and low contrast. (C) Mean microsaccade amplitude for each individual in each condition. The identity line represents equal amplitudes of high and low contrast. (D) Correlation between amplitudes of consecutive microsaccades. For the purpose of display, microsaccades were divided into 15 equidistant bins by size (*x* axis). Circles represent mean amplitude of the consecutive microsaccade, averaged across the microsaccades in each bin and across participants. Error bars denote the standard errors across participants. (E) Correlation between microsaccade amplitude and the following inter microsaccade interval. Microsaccades were divided into 15 equidistant bins by size (*x* axis). Circles represent mean inter microsaccade interval until the next saccade. Error bars denote the standard errors across participants.

high contrast: 1.23 Hz, low contrast: 1.25 Hz; $t(10) = 0.44$, $p = 0.66$.

Microsaccade amplitudes

The difference between conditions in saccade amplitudes (Figure 4C) was significant, $t(10) = 3.42$, $p = 0.0065$, with smaller amplitudes for the high-contrast condition (0.37° ± 0.09° vs. 0.41° ± 0.11°). The correlations between amplitudes of pairs of consecutive saccades (Figure 4D) were significantly positive across participants in both conditions—high contrast: mean $r = 0.29$, $t(10) = 7.03$, $p < 0.001$; low contrast: mean $r = 0.29$, $t(10) = 8.78$, $p < 10^{-5}$ (see individual correlations in Table 1): Smaller microsaccades tended to be followed by smaller microsaccades. The qualitative findings were also obtained after excluding SWJs—difference between displays: $t(11) = 3.76$, $p = 0.0037$; amplitude–amplitude correlations—high contrast: mean $r = 0.20$, $t(11) = 6.85$, $p < 10^{-4}$; low contrast: mean $r = 0.18$, $t(11) = 7.82$, $p < 10^{-4}$.

Correlation between amplitudes and IMSIs

As in Experiments 1 and 2, the correlations between saccade amplitude and the following IMSI (Figure 4E) were significantly negative across participants—high contrast: mean $r = -0.24$, $t(10) = 7.27$, $p < 0.001$; low contrast: mean $r = -0.24$, $t(10) = 9.45$, $p < 0.001$ (see individual correlations in Table 1). This indicates a tendency for longer IMSIs following smaller microsaccades and vice versa.

As in Experiment 2, a complementary analysis was performed to determine whether the effect of display on

IMSI is a direct consequence of its effect on microsaccade amplitudes, combined with the correlation of amplitude and IMSI, or whether it is an independent effect. The 95% confidence interval produced by the iterative procedure was [–12.6, 2.11], which included the zero value. We therefore conclude that there is no evidence for difference in the fitted μ values between the two displays. This null effect supports the claim that the effect of display on IMSI was mediated by its effect on microsaccade amplitudes.

Summary

Experiment 3 showed that with a background display of higher contrast, microsaccades were smaller and IMSIs longer. Consistent with the previous experiments, smaller microsaccades tended to be followed by smaller microsaccades and more prolonged IMSIs. Evidence supports a nondirect link between display properties and IMSIs, mediated by microsaccade amplitude.

Experiment 4

Experiments 1–3 established that the properties of the visual display modulate the parameters of the IMSI distribution, most likely through modulation of microsaccade amplitudes. However, the source of this relation remains undetermined. Microsaccades involve a displacement of the retinal image, which results in new input to the visual system. The purpose of Experiment 4 was to examine the role of the retinal-image displacement in the observed SRP effects. To examine this question, we relied on the horizontal directional bias of microsaccades (Nachmias, 1961; Engbert & Kliegl, 2003) and presented participants with vertical and horizontal grating displays (Figure 5A). Since most microsaccades are horizontal, a smaller average retinal displacement for horizontal than for vertical gratings displays is expected. We therefore predicted that the SRPs (measured by μ) would be longer for vertical than for horizontal grating orientations.

Saccade properties

Saccades followed the main sequence for all participants (correlation between amplitude and velocity: mean $r = 0.95$, $r > 0.84$ for all data sets). The mean saccade amplitude across observers was 0.38° ($SD =$ 0.14°), and nearly all saccades (97.4%) were defined as microsaccades (smaller than 1.5°). Importantly for the purpose of this experiment, the microsaccades demonstrated a horizontal direction bias, reflected by more horizontal than vertical microsaccades—horizontal: $M = 2{,}301$, $SD = 703$; vertical: $M = 871$, $SD = 727$; $t(12) = 4.48$, $p < 0.001$ (Figure 5B). The average number of analyzed microsaccades for an individual dataset was 3,046 ($SD = 836$, range = 1,286–4,215).

Distribution of IMSIs

The ex-Gaussian distribution showed the highest mean GOF (lowest BIC) across observers ($M = 8.55 \times 10^3$, $SD = 2.88 \times 10^3$), compared with an exponential distribution ($M = 1.02 \times 10^4$, $SD = 1.74 \times 10^3$, $p < 10^{-5}$), a Gaussian distribution ($M = 1.00 \times 10^4$, $SD = 1.62 \times 10^3$, $p < 10^{-5}$), and a gamma distribution ($M = 1.04 \times 10^4$, $SD = 1.64 \times 10^3$, $p < 0.001$).

Display effects on IMSIs

A 2×2 repeated-measures ANOVA was performed on the μ values of the fitted ex-Gaussian distribution, with factors spatial frequency (high/medium) and orientation (horizontal/vertical). This analysis confirmed our hypothesis by showing a significant main effect of orientation resulting from higher μ values for vertical than for horizontal gratings, $F(1, 12) = 5.57$, $p = 0.036$ (Figure 5C). Findings were consistent with the results of Experiment 2 in showing a main effect of SF, resulting from higher μ values for high than for medium SF, $F(1, 12) = 10.55$, $p = 0.007$ (Figure 5D). There was no evidence for a SF × Orientation interaction, $F(1, 12) = 1.3$, $p = 0.27$.

As for the previous experiments, we examined whether the effects on IMSIs can be explained by modulations of microsaccade rate. There was no evidence for an effect of orientation on microsaccade rate, $F(1, 12) = 0.191$, $p = 0.67$, but there was a marginally significant effect of SF, $F(1, 12) = 4.67$, $p = 0.051$, resulting from a higher microsaccade rate for lower SF. To examine whether the SF effect found for the μ parameter can be explained by this small effect of microsaccade rate, we correlated the difference between high and medium SF in saccade rates and in the μ parameters across participants. The same analysis was performed for the orientation conditions (correlating the difference between vertical and horizontal in saccade rates and μ parameters). There was no evidence for a correlation in either analysis—SF: $r(11) = -0.28$, $p = 0.34$; orientation: $r(11) = 0.12$, $p = 0.69$. We conclude that the effects of display condition on SRP duration (μ) are unlikely to be explained by differences in microsaccade rate.

Microsaccade amplitudes

We examined the effects of displays on microsaccade-amplitudes by performing a 2×2 repeated-measures ANOVA with the same factors as before.

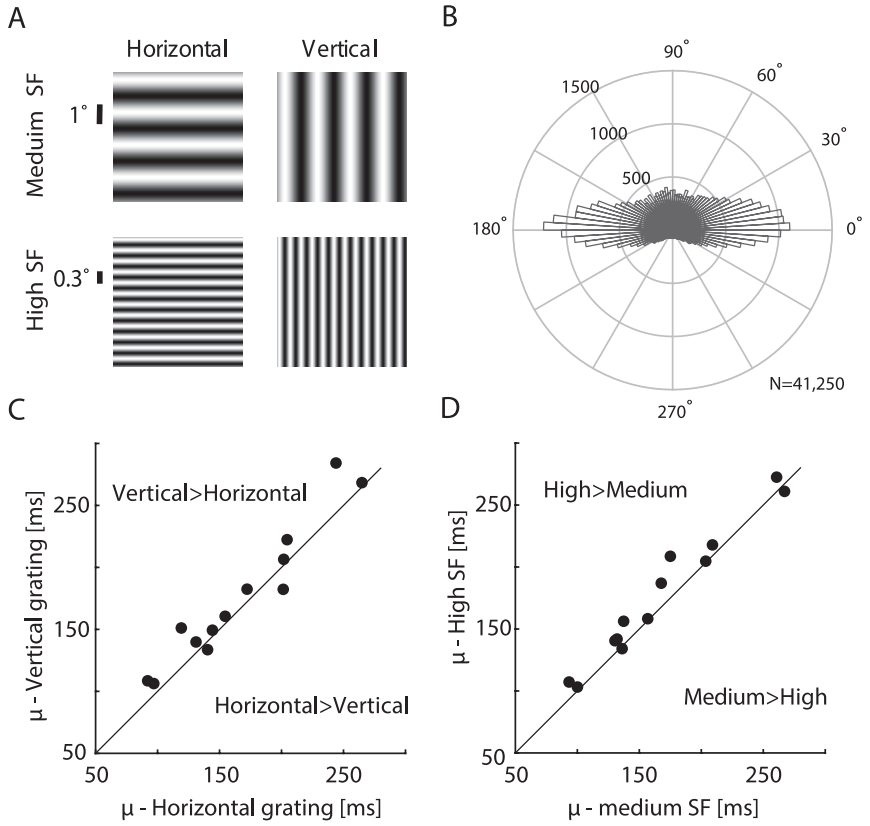

Figure 5. Summary of results for Experiment 4. (A) Display stimuli. (B) Spatial distribution of microsaccades. (C) Fitted μ parameter for each individual in horizontal- versus vertical-orientation displays. The identity line represents equal μ values for vertical and horizontal orientations. (D) Fitted μ parameter for each individual in high- versus medium-spatial-frequency displays. The identity line represents equal μ values for high and medium spatial frequency.

There was a significant main effect of orientation, $F(1, 12) = 7.52$, $p = 0.018$ (Figure 6A), resulting from smaller amplitudes for the vertical than for the horizontal orientation displays, and a main effect of SF, $F(1, 12) = 6.49$, $p = 0.026$, resulting from smaller amplitudes for the high-SF than for the medium-SF display (Figure 6B). There was no significant interaction ($F < 1$). The correlations between the amplitudes of pairs of consecutive saccades were significantly positive in all conditions across participants (Figure 6C)—vertical, high SF: mean $r = 0.35$, $t(12) = 8.04$, $p < 10^{-5}$; vertical, medium SF: mean $r = 0.33$, $t(12) = 8.03$, $p < 10^{-5}$; horizontal, high SF: mean $r = 0.33$, $t(12) = 8.18$, $p < 10^{-5}$; horizontal, medium SF: mean $r = 0.34$, $t(12) = 8.05$, $p < 10^{-5}$ (see individual correlations in Table 1).

Correlation between amplitudes and IMSIs

As in Experiments 1–3, the correlations between microsaccade amplitudes and the following IMSI (Figure 6D) were significantly negative across participants—vertical, high SF: mean $r = -0.15$, $t(12) = 3.41$, $p = 0.0051$; vertical, medium SF: mean $r = -0.17$, $t(12) = 5.14$, $p < 10^{-3}$; horizontal, high SF: mean $r = -0.15$, $t(12) = 4.07$, $p = 0.0015$; horizontal, medium SF: mean $r = -0.16$, $t(12) = 4.40$, $p < 10^{-3}$ (see individual correlations in Table 1). This indicates that smaller microsaccades tended to be followed by longer IMSIs.

Furthermore, as in the previous experiments, we examined whether the μ effects prevail on a data set that is balanced for microsaccade amplitudes. We constructed 95% confidence intervals on this balanced data set, separately for the SF and orientation effects. Zero was not included in either interval (SF effect: [2.67, 9.77]; orientation effect: [0.65, 7.23]), supporting the existence of independent effects of SF and orientation on the SRP regardless of amplitude.

Summary

This experiment replicated the SF effects of Experiment 2, with both the SRPs and microsaccade amplitudes. Additionally, findings show that the SRP was longer and microsaccades smaller for vertical relative to horizontal orientations. Together with the finding that there were many more horizontal than vertical microsaccades, these findings support the involvement of retinal-image displacements in inducing

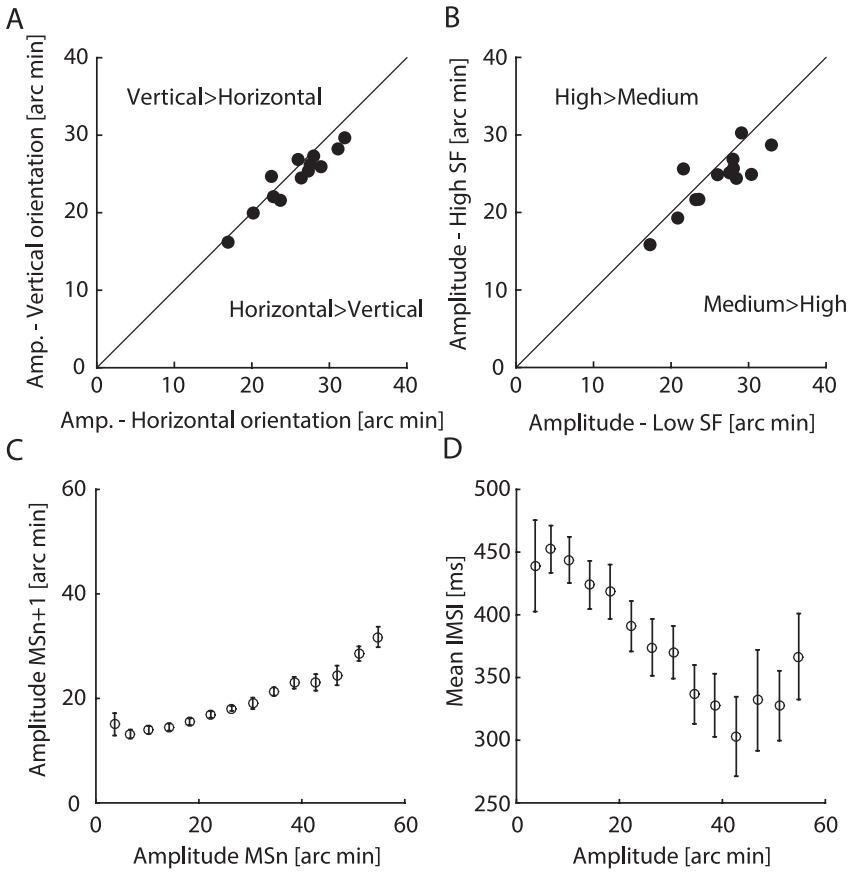

Figure 6. Amplitude results of Experiment 4. (A) Mean microsaccade amplitude for each individual in horizontal- versus vertical-orientation displays. The identity line represents equal amplitudes of vertical and horizontal orientations. (B) Mean microsaccade amplitude for each individual in high- versus medium-spatial-frequency displays. The identity line represents equal amplitudes for high and medium spatial frequency. (C) Correlation between amplitudes of consecutive microsaccades. For the purpose of display, microsaccades from all conditions were divided into 15 equidistant bins by size (*x* axis). Circles represent mean amplitude of the consecutive microsaccade, averaged across the microsaccades in each bin and across participants. Error bars denote the standard errors across participants. (D) Correlation between microsaccade amplitude and the following inter microsaccade interval. Microsaccades from all conditions were divided into 15 equidistant bins by size (*x* axis). Circles represent mean inter microsaccade interval until the next saccade. Error bars denote the standard errors across participants.

both effects. However, with this design we cannot exclude the involvement of other, nontransient, factors in contributing to the observed effects. For example, it is possible that the visual system reacts differently when exposed for prolonged durations to horizontal relative to vertical stimulation, and this results in changes of the duration between consecutive saccades.

Computational model

We compared the original model by Sinn and Engbert (2016) and our revised computational model (see Materials and methods) by testing the performance of both against the empirical data of Experiment 2. The set of parameters for each participant and condition was chosen by an extensive search (see Materials and methods). None of the parameters were found in the upper or lower bounds of the searched range. The chosen parameters ($M \pm SD$) were $E_{crit} = 7.89 \pm 0.02$, $\mu_0 = 141 \pm 31$, $\sigma = 40 \pm 23$, and $\mu_{ret} = 21.6 \pm 24.5$ (in the high-SF condition). The revised model showed a significantly better fit to the empirical data than the original model (revised model: mean $\chi^2 = 0.181$, $SD = 0.12$; original model: mean $\chi^2 = 2.08$, $SD = 0.83$), $t(22) = 7.21$, $p < 10^{-6}$.

Additionally, we compared the two models to theoretical distributions: Using the parameters of each participant, we produced two simulated data sets, one for each model. We then calculated the BIC for GOF (Kass & Raftery, 1995) of the simulated data with the theoretical gamma and ex-Gaussian distributions for each data set. The simulation data produced by the revised model showed a better fit (higher mean GOF and lower BIC) to the ex-Gaussian (mean BIC $= 5.24 \times 10^4$, $SD = 520$) than the gamma distribution (mean BIC

$= 5.28 \times 10^4$, $SD = 529$), $t(11) = 47.8$, $p < 10^{-14}$, resembling the empirical data. In contrast, the simulation data sets produced by the original model showed the opposite effect: a better fit to the gamma distribution (mean BIC $= 7.25 \times 10^4$, $SD = 359$) than the ex-Gaussian distribution (mean BIC $= 7.266 \times 10^4$, $SD = 368$), $t(11) = -11.2$, $p < 10^{-6}$. This suggests that the revised model is more consistent with the empirical data than is the original model.

Discussion

This study examined the effects of the properties of static displays on the generation of microsaccades. The findings show that more intense displays (i.e., higher contrast and SF) bring about smaller microsaccades and longer SRPs. Additionally, the amplitude of a microsaccade is negatively correlated with the duration of time until the next microsaccade (smaller microsaccades are followed by later microsaccades) and positively correlated with the next microsaccade's amplitude (smaller microsaccades are followed by smaller microsaccades). We discuss how these findings can be integrated into existing models of microsaccade generation, by taking into account the effects of the visual transients produced at the offsets of microsaccades.

Integrating the findings into the common-field model

The effects of the display could either be sustained, due to a general perceptual state related to the task or properties of the presented display, or transient, due to eye movements which are a source of transient visual changes that are determined by the properties of the display. Microsaccades shift the retina and create visual transients at their offsets. Studies in humans and animals have shown that these visual transients are processed by the visual system similar to those produced by the presentation of external stimuli (Kazai & Yagi, 2003; Dimigen, Valsecchi, Sommer, & Kliegl, 2009; Tse et al., 2010). Previous models of microsaccade generation have investigated the effects of external stimuli extensively (Rolfs, Kliegl, & Engbert, 2008; Rolfs, Laubrock, & Kliegl, 2008; Hafed & Ignashchenkova, 2013; Sinn & Engbert, 2016), but they do not account for the sustained effects of static displays or for the effects of the visual transients produced by the ongoing microsaccades performed on these displays. Furthermore, most previous studies on the effects of display on microsaccades have focused more on spatial aspects of microsaccades and less on how the display modulates their timings (e.g., McCamy et al., 2014).

One conceptual model is the common-field model proposed by Rolfs, Kliegl, and Engbert (2008), which explains microsaccade generation as a consequence of local excitation in oculomotor maps of the superior colliculus. This excitation is thought to spread slightly around the center of the map and generate microsaccades when it crosses a certain threshold. This idea was physiologically verified by later findings showing that microsaccades are associated with activity near the rostral pole of the superior colliculus (Hafed et al., 2009). The inhibition of microsaccades following the abrupt onset of a stimulus is explained by this model as the result of global inhibition in this map produced by the visual transient at the onset of the stimulus. This model is powerful in explaining various phenomena related to the generation of microsaccades, but it does not account for the effects of the low-level properties of the display and for the effects of each microsaccade on the generation of subsequent microsaccades.

In the present study we filled this gap by examining how microsaccade generation is modulated by the properties of the static display on which they are produced (sustained effects) and how the properties of one microsaccade modulate the next (transient effects). We outline our findings and propose conceptual frameworks for integrating each of them into the common-field model of microsaccade generation.

The sustained effect of display: Microsaccades produced on more intense displays are smaller

Microsaccades produced on displays of higher SF and contrast tend to be smaller. We hypothesize that this effect is due to the lateral inhibitory connections which continuously normalize activity across the map (Munoz & Istvan, 1998). According to this view, the sustained exposure to a large and intense visual display results in elevated activation in all areas of the superior colliculus mapping this stimulus. Since the center of the map is smaller than its periphery, and activity is normalized across the map, stronger global activity results in weaker relative activity at the center of the map (Figure 7A). With this weaker central activity, only locations which are very close to the center of fixation could cross the threshold for saccade generation. Consequently, with more intense displays the produced microsaccades tend to be smaller. This hypothesis is illustrated in Figure 7A.

The transient effect of one microsaccade on the next one: Smaller microsaccades are followed by smaller and later microsaccades

We found that the amplitude of one microsaccade is negatively correlated with the duration of time until the next microsaccade (small microsaccades are followed

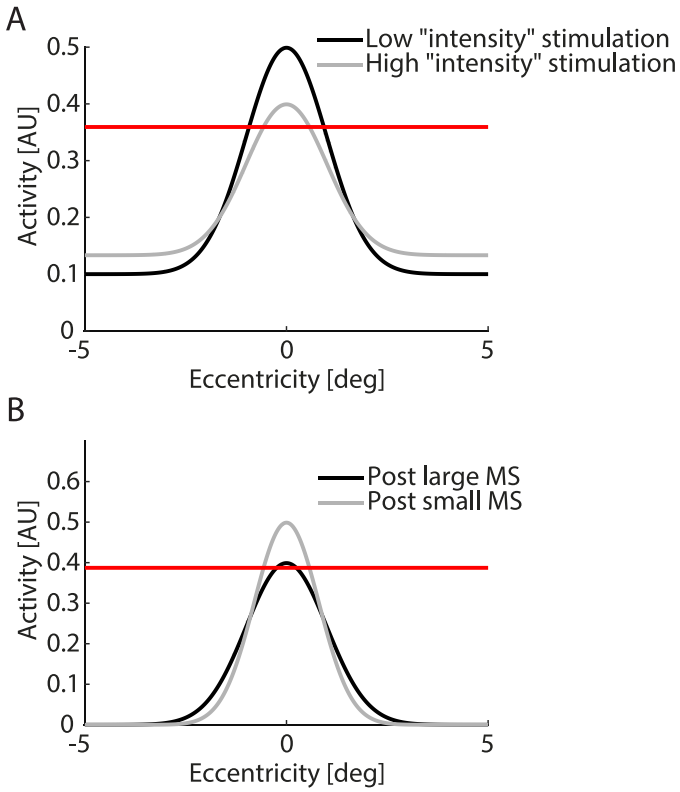

Figure 7. Schematic demonstration of the distribution of activity in the superior colliculus motor map according to the proposed model, based on the common-field model. The *x* axis represents the eccentricities of map location relative to the center of fixation (at zero). The *y* axis represents activity in arbitrary units (AU). (A) Sustained activity in the superior colliculus map for stimuli of higher or lower intensities. Activity is normalized, and therefore areas under the curve are equal regardless of the stimulus. With the high-intensity stimulus, activity in the center is weaker relative to the periphery and microsaccades are likely to be smaller. (B) Transient effect of small and large microsaccades on map activity. Smaller microsaccades produce smaller visual transients and consequently smaller central perturbation in the map, and vice versa for larger microsaccades.

by long IMSIs) and positively correlated with the amplitude of the next microsaccade (small microsaccades are followed by small microsaccades). These effects are time-locked to the microsaccades themselves and are therefore, by definition, the result of transient rather than sustained activity. We hypothesize that these transient effects are caused by the retinal-image displacements produced at the offset of each microsaccade.

Smaller microsaccades produce smaller retinal displacements than larger microsaccades. Therefore, a small microsaccade is expected to create only a small perturbation in central locations of the map, close to the rostral pole. In contrast, larger microsaccades produce larger perturbations in central locations which are slightly less focused at the center than those produced by smaller microsaccades. When central activity is more focal and weaker, such as after a small microsaccade, the next microsaccade will tend be small and will take more time to produce; when central activity is stronger and slightly less central, such as after a large microsaccade, the next microsaccade will tend to be large and will take less time to produce. This is demonstrated in Figure 7B.

The involvement of visual transients caused by the retinal-image change in determining the amplitudes and latency of subsequent microsaccades is established by two of the present findings: First, in experimental conditions designed to induce weaker visual transients (such as in Experiment 1's darkness conditions and Experiment 4's horizontal-grating conditions), saccades were larger and the SRP shorter than in conditions which induced stronger visual transients. Second, in the darkness free-view condition of Experiment 1, where no visual transient accompanied the saccades, no link between amplitude and IMSI was found.

Rolfs, Laubrock, and Kliegl (2008) found what seems to be an opposite finding to the present one: After smaller microsaccades, response times of voluntary saccades were shorter than those following larger microsaccades. This finding may seem to contradict our finding of longer SRPs following smaller microsaccades, but it is in fact perfectly consistent with it. The difference between the previous study and the present one is that Rolfs and colleagues examined response times of large voluntary saccades, whereas we examined the SRPs between microsaccades. According to Rolfs and colleagues, smaller microsaccades are associated with weaker central activity, which results in lower competition between center and periphery and consequently shorter intervals until a large saccade can be produced. But in addition to making larger saccades *more* probable, this smaller central activity may render the production of microsaccades *less* probable. This is reflected in our finding of longer intervals until the next microsaccade can be produced. Therefore, the amplitude of a preceding microsaccade is expected to induce opposite effects on the timing of subsequent large saccades and microsaccades. Consistent with this interpretation, in Experiment 1 we show that the amplitude of a microsaccade is negatively correlated with the duration of time until the next microsaccade (in a fixation task) and positively correlated with the duration of time until the next large saccade (in a free-view task).

In explaining the association between central map activation and the amplitudes of microsaccades, Rolfs and colleagues suggest that weaker central activity results in smaller microsaccades and stronger central activity results in larger microsaccades. By integrating the effects of the visual transients into the common-field model, we suggest that a fuller picture of micro-

saccade production can be obtained. According to this view, smaller microsaccades produce smaller visual transients, which in turn produce weaker central activity and smaller microsaccades; and vice versa for larger microsaccades. Therefore, the amplitude of activity at the center of the map is not only the *cause* but also the *consequence* of the sizes of the microsaccades that are being produced.

The SRP is longer for more intense displays

Additionally, we found that with more intense displays, the SRP between consecutive microsaccades is longer. We hypothesize that the effect of display SF on the SRP is a consequence of the visual transient produced at the offset of each microsaccade: When the SF of the display is higher, this transient is more intense and results in a longer refractory period until the next microsaccade. For the SF modulation we found this effect to be independent of microsaccade amplitudes, suggesting a direct link between the SF of the visual transient at the offset of one microsaccade and the time until the next microsaccade. For the contrast modulation we found no evidence of an independent effect, suggesting that the link between the visual transients and the SRP is indirect: Higher contrast produces smaller microsaccades which, in turn, tend to be followed by longer SRPs. Regardless of whether the link between the display properties and the SRP is direct or mediated by microsaccade amplitudes, it is likely to be the consequence of the transient effect of each single microsaccade.

The role of the visual transients produced by microsaccades on the timings of subsequent microsaccades

Our findings demonstrate both the sustained effects of the visual displays and the transient effects of microsaccades produced on these displays: The display properties have a sustained effect on the amplitudes of microsaccades (more intense displays result in smaller microsaccade), and each microsaccade has a transient effect on the timing of the next one (smaller microsaccades and microsaccades that are performed on displays of higher SF result in a longer interval until the next microsaccade). The latter, according to our view, is the result of the retinal-image displacement, which creates a visual transient at microsaccade offset. According to this view, the visual transient induced by each microsaccade is not only the consequence of that specific microsaccade but also an important factor in determining the timings of subsequent microsaccades and consequently in determining the general temporal dynamics of microsaccade generation. The implication of this is that microsaccade generation depends on a loop in which each microsaccade is determined (among other factors) by the visual consequence of the previous one.

Importantly, despite attributing such a central role to the visual transients produced by microsaccades, this view does not underestimate the important contribution of other factors, such as the sustained effects of the display and top-down effects, on determining the timings of microsaccades. Clearly, specific goals, attentional demands, and the perceptual context modulate the timing of saccades and microsaccades considerably. Our hypothesis adds to these top-down contributions the claim that bottom-up effects, driven by the display and the visual transients, may also be a substantial contributing factor in determining the temporal dynamics of microsaccades.

Implications for models of microsaccade generation

The common-field model provides an extended account of the spatial aspects of microsaccade generation, but it remains inconclusive in explaining some of its temporal aspects. According to Rolfs, Kliegl, and Engbert (2008), central activity during fixations may be above threshold at any time, and a temporal trigger is therefore required to account for the rate of microsaccades during fixation. They suggest three possible temporal triggering mechanisms: noise in the oculomotor map activity, which may shift the balance of the oculomotor maps and fluctuate activity around the threshold for saccadic generation; variability of the visual input signals produced by eye movements, such as ocular drift (Engbert & Mergenthaler, 2006; Engbert et al., 2011); and an autonomous timing mechanism for saccade generation (Trukenbrod & Engbert, 2014; Hogendoorn, 2016), which may or may not depend on the changing oculomotor needs. These needs may include, for instance, top-down task-related effects such as the tendency to correct fixation errors imposed by the fixation task (Krauzlis, Basso, & Wurtz, 1997) or a drive to explore fine details imposed by other tasks (Ko et al., 2010).

The present findings show a link between the characteristics of a static display and the timings of microsaccades produced on it. We hypothesize that the visual input produced by eye movements on the constant displays, and specifically produced by the microsaccades themselves, has a central role in determining the temporal dynamics of subsequent microsaccades (the second of the options suggested by Rolfs and colleagues). In a previous study (Amit et al., 2017) we showed that saccade sequences feature only first-order and no high-order temporal dependencies:

Each saccade depends solely on the single preceding saccade and not on a longer sequence of previous saccades. We further showed that the SRP is the source of the first-order interdependency between consecutive saccades, and its duration and variability determine their rhythmic modulation. Using a simple simulation model, we demonstrated how the timing and rhythmic characteristics of saccades can be produced solely by a stochastic process which is constrained by a Gaussian SRP. According to this view, saccades are not paced by an external pacemaker but are self-paced: Each saccade is a link in a chain of neural processes which eventually drive the next saccade. Therefore, in addition to their inherent randomness (the first option) and subject to their dependency on the consequences of previous oculomotor events (second option), saccades are not driven by an autonomous generator (as in the third option) but are a self-paced process.

Here we suggest that the visual transients which are produced by one microsaccade determine the timing of the next and are therefore a critical factor in the self-generating chain of microsaccade generation. Specifically, the SRP is modulated by the characteristics of the display: by both the sustained effects of the display and the transient effects of the preceding microsaccades. We suggest that integrating these microsaccade-induced transient effects into models of microsaccade generation would not be a mere technical addition to these models but would reflect a novel conceptualization of microsaccade generation as a self-generating process, where microsaccades are driven (among other factors) by consequences of previous oculomotor events. Indeed, we find that the temporal predictions of the computational model by Engbert et al. (2011) fit the data better when the effects of the visual transients—that is, a context-dependent Gaussian refractory period resulting in an ex-Gaussian distribution of intervals—are integrated into it.

Is the SRP linked to the inhibition of saccades following a stimulus?

It is well established that visual transients caused by the external display of a stimulus produce a short (approximately 150–200 ms) inhibition of saccades and microsaccades, which is sometimes followed by a rebound. It is a reasonable conjecture that this stimulus-related inhibition of saccades can be induced not only by external stimulation but also by the visual transient produced by the saccades themselves. Combining the known effects of the stimulus-related saccadic inhibition with the fact that saccades produce a visual transient provides a full account of the origins of the SRP. This hypothesis is supported by the highly similar temporal dynamics of the stimulus-related saccadic inhibition and the SRP: Event (saccade offset/stimulus onset) causes a temporary inhibition of saccade rate which then rebounds before returning to baseline.

This argument gets more complicated, however, considering the ambivalent findings regarding the direction of the link between the properties of the presented stimulus and the characteristics of the stimulus-related saccadic inhibition. Some researchers have found that poststimulus inhibition of microsaccades is deeper for stimuli of higher contrast (Scholes, McGraw, Nyström, & Roach, 2015; White & Rolfs, 2016). This may seem consistent with our finding of longer SRP for stimuli of higher contrast. However, other studies focusing on the duration of inhibition rather than its depth have shown an inconsistent (Rolfs, Kliegl, & Engbert, 2008) or even opposite (Bonneh, Adini, & Polat, 2015) relation—that is, shorter poststimulus inhibition for stimuli of higher contrast. Regarding spatial frequency, Bonneh et al. have shown that the link between the SF of the stimulus and the duration of inhibition following it depends on the specific properties of the stimulus: Stimuli of low SF (<2 c/°) showed a monotonic positive relation between SF and the duration of inhibition, but stimuli of higher SF (>2 c/°) showed the opposite trend. Despite the relatively low SF we used (our high SF was slightly lower than 2 c/°), our findings may reflect the descending arm of a U-shaped function. We conclude that more research is required for a fuller understanding of the link between SRP and stimulus-related inhibition.

Conclusions

The low-level features of the constant display modulate the amplitudes of microsaccades, which in turn modulate the intervals of time between them. Our conceptual model proposes that both sustained effects of constant display and transient effects caused by the retinal change entailed by each saccade are involved in determining the temporal dynamics of microsaccade generation, but an autonomous triggering mechanism is not necessary to explain them. The effect of the properties of the visual display and the influence of one microsaccade over the next have rarely been considered by previous models of saccade generation but play important roles in determining the timings of microsaccades.

Keywords: saccades, microsaccades, spatial frequency, contrast, eye movements, eye tracking, free view, fixation

Acknowledgments

This work was funded by ISF Grant 1427/14. We thank Avia Eyal for her assistance in running experiments, and Noam Tal and Rinat Hilo for fruitful discussions.

Commercial relationships: none.
Corresponding author: Shlomit Yuval-Greenberg.
Email: shlomitgr@tau.ac.il.
Address: Cognitive Neuroscience Lab, School of Psychological Sciences and Sagol School of Neuroscience, Tel Aviv University, Tel Aviv, Israel.

References

Ahissar, E., Arieli, A., Fried, M., & Bonneh, Y. (2016). On the possible roles of microsaccades and drifts in visual perception. *Vision Research*, *118*, 25–30.

Amit, R., Abeles, D., Bar-Gad, I., & Yuval-Greenberg, S. (2017). Temporal dynamics of saccades explained by a self-paced process. *Scientific Reports*, *7*:886.

Bahill, A. T., Clark, M. R., & Stark, L. (1975). The main sequence, a tool for studying human eye movements. *Mathematical Biosciences*, *24*, 191–204.

Bair, W., & Keefe, L. P. O. (1998). The inflence of fixational eye movements on the response of neurons in area MT of the macaque. *Visual Neuroscience*, *15*(4), 779–786.

Beeler, G. W. (1965). *Stochastic processes in the human eye movement control system*. Dissertation (PhD), California Institute of Technology.

Bonneh, Y. S., Adini, Y., & Polat, U. (2015). Contrast sensitivity revealed by microsaccades. *Journal of Vision*, *15*(9):11, 1–12, https://doi.org/10.1167/15.9.11. [PubMed] [Article]

Bosman, C. A., Womelsdorf, T., Desimone, R., & Fries, P. (2009). A microsaccadic rhythm modulates gamma-band synchronization and behavior. *The Journal of Neuroscience*, *29*, 9471–9480.

Carpenter, R. H. S. (1977). *Movements of the eyes*. London: Pion.

Carpenter, R. H. S., & Williams, M. L. L. (1995, September 7). Neural computation of log likelihood in control of saccadic eye movements. *Nature*, *377*(6544), 59–62.

Cousineau, D. (2005). Confidence intervals in within-subject designs: A simpler solution to Loftus and Masson's method. *Tutorials in Quantitative Methods for Psychology*, *1*, 42–45.

D'Agostino, R. B. (1986). *Goodness-of-fit techniques*. New York: CRC Press.

Dimigen, O., Valsecchi, M., Sommer, W., & Kliegl, R. (2009). Human microsaccade-related visual responses. *The Journal of Neuroscience*, *29*, 12321–12331.

Einhäuser, W., & König, P. (2003). Does luminance-contrast contribute to a saliency map for overt visual attention? *The European Journal of Neuroscience*, *17*, 1089–1097.

Engbert, R. (2012). Computational modeling of collicular integration of perceptual responses and attention in microsaccades. *The Journal of Neuroscience*, *32*, 8035–8039.

Engbert, R., & Kliegl, R. (2003). Microsaccades uncover the orientation of covert attention. *Vision Research*, *43*, 1035–1045.

Engbert, R., & Mergenthaler, K. (2006). Microsaccades are triggered by low retinal image slip. *Proceedings of the National Academy of Sciences, USA*, *103*, 7192–7197.

Engbert, R., Mergenthaler, K., Sinn, P., & Pikovsky, A. (2011). An integrated model of fixational eye movements and microsaccades. *Proceedings of the National Academy of Sciences, USA*, *108*, E765–E770.

Graupner, S. T., Velichkovsky, B. M., Pannasch, S., & Marx, J. (2007). Surprise, surprise: Two distinct components in the visually evoked distractor effect. *Psychophysiology*, *44*, 251–261.

Hafed, Z. M., & Clark, J. J. (2002). Microsaccades as an overt measure of covert attention shifts. *Vision Research*, *42*, 2533–2545.

Hafed, Z. M., Goffart, L., & Krauzlis, R. J. (2009, February 15). A neural mechanism for microsaccade generation in the primate superior colliculus. *Science*, *323*(5916), 940–943.

Hafed, Z. M., & Ignashchenkova, A. (2013). On the dissociation between microsaccade rate and direction after peripheral cues: Microsaccadic inhibition revisited. *The Journal of Neuroscience*, *33*, 16220–16235.

Hanes, D. P., & Schall, J. D. (1996, October 18). Neural control of voluntary movement initiation. *Science*, *274*(5286), 427–430.

Henderson, J. M. (2003). Human gaze control during real-world scene perception. *Trends in Cognitive Sciences*, *7*, 498–504.

Hogendoorn, H. (2016). Voluntary saccadic eye movements ride the attentional rhythm. *Journal of Cognitive Neuroscience*, *28*, 1625–1635.

Itti, L. (2005). Quantifying the contribution of low-

level saliency to human eye movements in dynamic scenes. *Visual Cognition*, *12*, 1093–1123.

Kagan, I., & Snodderly, D. M. (2017). Saccades and drifts differentially modulate neuronal activity in V1: Effects of retinal image motion, position, and extraretinal influences. *Journal of Vision*, *8*(14):19, 1–25, https://doi.org/10.1167/8.14.19. [PubMed] [Article]

Kass, R. E., & Raftery, A. E. (1995). Bayes factors. *Journal of the American Statistical Association*, *90*, 773–795.

Kazai, K., & Yagi, A. (2003). Comparison between the lambda response of eye-fixation-related potentials and the P100 component of pattern-reversal visual evoked potentials. *Cognitive, Affective & Behavioral Neuroscience*, *3*, 46–56.

Ko, H.-K., Poletti, M., & Rucci, M. (2010). Microsaccades precisely relocate gaze in a high visual acuity task. *Nature Neuroscience*, *13*, 1549–1553.

Krauzlis, R. J., Basso, M. A., & Wurtz, R. H. (1997, June 13). Shared motor error for multiple eye movements. *Science*, *276*(5319), 1693–1695.

Lacouture, Y., & Cousineau, D. (2008). How to use MATLAB to fit ex-Gaussian and other probability functions to a distribution of response times probability functions to a distribution of response times. *Tutorials in Quantitative Methods for Psychology*, *4*, 35–45.

Laubrock, J., Engbert, R., & Kliegl, R. (2005). Microsaccade dynamics during covert attention. *Vision Research*, *45*, 721–730.

Martinez-Conde, S., Macknik, S. L., & Hubel, D. H. (2004). The role of fixational eye movements in visual perception. *Nature Reviews Neuroscience*, *5*, 229–240.

McCamy, M. B., Otero-Millan, J., Di Stasi, L. L., Macknik, S. L., & Martinez-Conde, S. (2014). Microsaccade production during visual scanning. *The Journal of Neuroscience*, *34*, 2956–2966.

McCamy, M. B., Otero-Millan, J., Leigh, R. J., King, S. A., Schneider, R. M., Macknik, S. L., & Martinez-Conde, S. (2015). Simultaneous recordings of human microsaccades and drifts with a contemporary video eye tracker and the search coil technique. *PLoS One*, *10*(6):e0128428.

Meyberg, S., Sinn, P., Engbert, R., & Sommer, W. (2017). Revising the link between microsaccades and the spatial cueing of voluntary attention. *Vision Research*, *133*, 47–60.

Michelson, A. A. (1927). *Studies in optics*. Chicago: University of Chicago Press.

Munoz, D. P., Dorris, M. C., Pare, M., & Everling, S. (2000). On your mark, get set: Brainstem circuitry underlying saccadic initiation. *Canadian Journal of Physiology and Pharmacology*, *78*, 934–944.

Munoz, D. P., & Istvan, P. J. (1998). Lateral inhibitory interactions in the intermediate layers of the monkey superior colliculus. *Journal of Neurophysiology*, *79*, 1193–1209.

Nachmias, J. (1961). Determiners of the drift of the eye during monocular fixation. *Journal of the Optical Society of America*, *51*, 761–766.

Nasanen, R., Ojanpaa, H., & Kojo, I. (2001). Effect of stimulus contrast on performance and eye movements in visual search. *Vision Research*, *41*, 1817–1824.

Ojanpaa, H., Nasanen, R., & Kojo, I. (2002). Eye movements in the visual search of word lists. *Vision Research*, *42*, 1499–1512.

Otero-Millan, J., Serra, A., Leigh, R. J., Troncoso, X. G., Macknik, S. L., & Martinez-Conde, S. (2011). Distinctive features of saccadic intrusions and microsaccades in progressive supranuclear palsy. *The Journal of Neuroscience*, *31*, 4379–4387.

Otero-Millan, J., Troncoso, X. G., Macknik, S. L., Serrano-Pedraza, I., & Martinez-Conde, S. (2008). Saccades and microsaccades during visual fixation, exploration, and search: Foundations for a common saccadic generator. *Journal of Vision*, *8*(14):21, 1–18, https://doi.org/10.1167/8.14.21. [PubMed] [Article]

Poletti, M., & Rucci, M. (2016). A compact field guide to the study of microsaccades: Challenges and functions. *Vision Research*, *118*, 83–97.

Rayner, K. (1998). Eye movements in reading and information processing: 20 years of research. *Psychological Bulletin*, *124*, 372–422.

Reingold, E. M., & Stampe, D. M. (2002). Saccadic inhibition in voluntary and reflexive saccades. *Journal of Cognitive Neuroscience*, *14*, 371–388.

Robinson, D. A. (1972). Eye movements evoked by collicular stimulation in the alert monkey. *Vision Research*, *12*, 1795–1808.

Rolfs, M., Kliegl, R., & Engbert, R. (2008). Toward a model of microsaccade generation: The case of microsaccadic inhibition. *Journal of Vision*, *8*(11):5, 1–23, https://doi.org/10.1167/8.11.5. [PubMed] [Article]

Rolfs, M., Laubrock, J., & Kliegl, R. (2008). Microsaccade-induced prolongation of saccadic latencies depends on microsaccade amplitude. *Journal of Eye Movement Research*, *1*, 1–8.

Scholes, C., McGraw, P. V., Nyström, M., & Roach, N. W. (2015). Fixational eye movements predict

visual sensitivity. *Proceedings of the Royal Society B:Biological Sciences*, *282*(1817):20151568.

Silver, C., & Dunlap, W. (1987). Averaging correlation coefficents: Should Fisher's *z* transformation be used? *Journal of Applied Psychology*, *72*, 146–148.

Sinn, P., & Engbert, R. (2016). Small saccades versus microsaccades: Experimental distinction and model-based unification. *Vision Research*, *118*, 132–143.

Thickbroom, G. W., Knezevič, W., Carroll, W. M., & Mastaglia, F. L. (1991). Saccade onset and offset lambda waves: Relation to pattern movement visually evoked potentials. *Brain Research*, *551*, 150–156.

Trukenbrod, H. A., & Engbert, R. (2014). ICAT: A computational model for the adaptive control of fixation durations. *Psychonomic Bulletin and Review*, *21*, 907–934.

Tse, P. U., Baumgartner, F. J., & Greenlee, M. W. (2010). Event-related functional MRI of cortical activity evoked by microsaccades, small visually-guided saccades, and eyeblinks in human visual cortex. *NeuroImage*, *49*, 805–816.

Wang, D., Mulvey, F. B., Pelz, J. B., & Holmqvist, K. (2016). A study of artificial eyes for the measurement of precision in eye-trackers. *Behavior Research Methods*, *49*, 947–959.

White, A. L., & Rolfs, M. (2016). Oculomotor inhibition covaries with perceptual awareness. *Journal of Neurophysiology*, *116*, 1507–1521.

Yekutieli, D., & Benjamini, Y. (1999). Resampling-based false discovery rate controlling multiple test procedures for correlated test statistics. *Journal of Statistical Planning and Inference*, *82*, 171–196.

Yuval-Greenberg, S., Merriam, E. P., & Heeger, D. J. (2014). Spontaneous microsaccades reflect shifts in covert attention. *The Journal of Neuroscience*, *34*, 13693–13700.

Zuber, B. L., Stark, L., & Cook, G. (1965, December 10). Microsaccades and the velocity-amplitude relationship for saccadic eye movements. *Science*, *150*(3702), 1459–1460.